

Journal of Visualized Experiments

Studying Triple Negative Breast Cancer Using Orthotopic Breast Cancer Model

--Manuscript Draft--

Article Type:	Invited Methods Article - JoVE Produced Video
Manuscript Number:	JoVE60316R3
Full Title:	Studying Triple Negative Breast Cancer Using Orthotopic Breast Cancer Model
Section/Category:	JoVE Cancer Research
Keywords:	MDA-MB-231 orthotopic metastasis breast cancer TNBC
Corresponding Author:	Robert Yuk Sing Cheng, D.V.M., Ph.D. NCI at Frederick Frederick, MD UNITED STATES
Corresponding Author's Institution:	NCI at Frederick
Corresponding Author E-Mail:	ryscheng@gmail.com
Order of Authors:	Robert Yuk Sing Cheng, D.V.M., Ph.D. Nimit L Patel Timothy Back Debashree Basudhar Veena Somasundaram Joseph D Kalen David A. Wink Lisa A. Ridnour
Additional Information:	
Question	Response
Please indicate whether this article will be Standard Access or Open Access.	Open Access (US\$4,200)
Please indicate the city, state/province, and country where this article will be filmed . Please do not use abbreviations.	Frederick, MD, USA



DEPARTMENT OF HEALTH & HUMAN SERVICES

Public Health Service

National Institutes of Health
Bethesda, Maryland 20892www.nih.gov

5/24/2019

Dear JoVE Editor:

We are submitting our manuscript, entitled **"A Practical Guide to Study Triple Negative Breast Cancer Using Orthotopic Breast Cancer Model"** to be considered for publication in JoVE. The manuscript is an original work, has not been previously published, and is not under consideration for publication elsewhere.

We previously utilized the orthotopic breast cancer model for our breast cancer metastasis studies (Basudhar *et al* J Med Chem 2013; Heinecke *et al* PNAS 2014, Cheng *et al* Nitric Oxide 2014; Basudhar *et al* FRBM 2015). In this manuscript, we provide detailed steps of establishing an orthotopic breast cancer model. We demonstrate the practical guidance for cell line preparation, tumor burden measurement, in vivo imaging, ex vivo imaging, metastatic lung lesion assessment, and molecular detection/validation. In addition, we provide suggestions on validation of imaging data, data analysis as well as data interpretation. This manuscript is able to guide the researchers who are interested in setting up an orthotopic breast cancer model for the assessment of therapeutic efficacy. Overall, it helps in developing therapeutic agents against breast cancer especially metastasis.

All authors have read the manuscript, agreed that the work is ready for submission to JoVE, and accepted the responsibility for the manuscript's contents. We declare that we have no competing financial interests.

Thank you for considering our manuscript for publication in the JoVE.

Yours sincerely,

A handwritten signature in black ink, appearing to read "Robert Cheng".

Dr. Y.S. Robert Cheng, D.V.M., Ph.D.
Molecular Mechanisms Section,
Cancer and Inflammation Program,
Center for Cancer Research,
National Cancer Institute,
Office: Building 576 Room 109
Lab: Building 567 Room 275
1050 Boyles Street,
Frederick, MD 21702-1201
Phone: (301) 228-4386

TITLE:**Studying Triple Negative Breast Cancer Using Orthotopic Breast Cancer Model****AUTHORS AND AFFILIATIONS:**

Robert Y. S. Cheng¹, Nimit L. Patel², Timothy Back¹, Debashree Basudhar¹, Veena Somasundaram¹, Joseph D. Kalen², David A. Wink¹, Lisa A. Ridnour¹

¹Molecular Mechanism Section, Cancer and Inflammation Program, Center for Cancer Research, National Cancer Institute at Frederick, Frederick, MD, USA

²Frederick National Laboratory for Cancer Research, Small Animal Imaging Program, Leidos Biomedical Research, Inc., Frederick, MD, USA

Corresponding Author:

Lisa A. Ridnour (ridnourl@mail.nih.gov)

Email Addresses of Co-authors:

Robert Y. S. Cheng (robert.cheng2@nih.gov)

Nimit L. Patel (nimit.patel@nih.gov)

Timothy Back (backt@mail.nih.gov)

Debashree Basudhar (debashree.basudhar@nih.gov)

Veena Somasundaram (veena.somasundaram@nih.gov)

Joseph D. Kalen (kalenj@mail.nih.gov)

David A. Wink (wink@mail.nih.gov)

KEYWORDS:

MDA-MB-231, orthotopic, metastasis, breast, cancer, TNBC

SUMMARY:

This work presets an advanced protocol to accurately assess tumor loading by detection of green fluorescent protein and bioluminescence signals as well as the integration of quantitative molecular detection technique.

ABSTRACT:

Triple-negative breast cancer (TNBC) is an aggressive breast cancer subtype with limited therapeutic options. When compared to patients with less aggressive breast tumors, the 5-year survival rate of TNBC patients is 77% due to their characteristic drug-resistant phenotype and metastatic burden. Toward this end, murine models have been established aimed at identifying novel therapeutic strategies limiting TNBC tumor growth and metastatic spread. This work describes a practical guide for the TNBC orthotopic model where MDA-MB-231 breast cancer cells suspended in a basement membrane matrix are implanted in the fourth mammary fat pad, which closely mimics the cancer cell behavior in humans. Measurement of tumors by caliper, lung metastasis assessment via in vivo and ex vivo imaging, and molecular detection are discussed. This model provides an excellent platform to study therapeutic efficacy and is

especially suitable for the study of the interaction between the primary tumor and distal metastatic sites.

INTRODUCTION:

Approximately one in eight women in the United States will develop invasive breast cancer during her lifetime, and 10%–20% of these women will be diagnosed with the aggressive triple negative breast cancer (TNBC) subtype. While primary lesions can be surgically removed in most cases, the subclinical micrometastasis and chemoresistance make it an intractable disease. Importantly, most patients with metastatic TNBC eventually relapse, even if they underwent treatment in the early stage¹. Thus, cancer heterogeneity, micrometastasis, and therapeutic resistance are three major challenges limiting the successful clinical outcome of TNBC patients. Hence, there is an urgent need to better understand the polymorphic molecular background of TNBC and develop effective therapeutic agents that limit metastatic disease.

Tumor metastasis is a multistep process where the tumor cell controls and usurps its microenvironment to promote its own dissemination via membrane degradation and tumor cell escape from the primary lesion, via entry into (i.e., intravasation) and exit from (i.e., extravasation) the vasculature, and ultimately adaptation and colonization within distal tissue beds². Animal models have been developed to study breast cancer metastasis, where two methodologies are commonly implemented: direct blood circulation injection and orthotopic implantation. Commonly employed methods for direct blood circulation injection include tail vein injection, while other approaches including direct cardiac injection³, direct brain injection⁴, and direct liver injection⁵ have also been employed. The direct blood circulation injection is often referred to as an artificial metastasis model, which is quick and easy but less physiologically accurate because it circumvents tumor escape from the primary lesion and intravasation⁶⁻⁸. When compared to direct injection models, the orthotopic breast cancer model takes longer for the occurrence of detectable metastatic lesions in remote organs such as the lung, but it is more physiologically relevant because it closely mimics the multistep metastatic process as it occurs in humans. Importantly, a 2013 study⁹ compared the tail vein injection and orthotopic models and found that the breast cancer cells injected into the tail vein and those isolated from lung metastatic lesions after tail vein injection exhibited similar global gene expression profiles. In contrast, the global gene expression profile of orthotopically injected breast cancer cells was dramatically different than that of lung metastatic lesions arising from orthotopically injected cells⁹. These observations suggest that the orthotopic model is more physiologically relevant, because the metastatic lesions undergo a selection process similar to the multistep process of metastasis as it occurs in humans.

This work describes an orthotopic breast cancer (MDA-MB-231-Luc/GFP) model in nude mice that was optimized in our laboratory for imaging detection techniques as well as the identification of novel biomarkers and development of targeted chemotherapeutic agents.

PROTOCOL:

Analysis of tumor growth was carried out using protocols approved by the Committee for the Ethics of Animal Experiments of the National Cancer Institute and adhered to the recommendations of the United States National Research Council's "Guide for the Care and Use of Laboratory Animals", the United States Public Health Service's "Guide for the Care and Use of Laboratory Animals", and the "Policy on Humane Care and Use of Laboratory Animals".

1. Preparation of cells for implantation

NOTE: MDA-MB-231 human breast adenocarcinoma cells (commercially acquired) were stably transfected with the luciferase gene III and enhanced green fluorescent protein (GFP) marker by lentivirus and grown in the presence of the selection antibiotic (puromycin).

1.1. Start the cell culture with 1×10^6 MDA-MB-231-Luc/GFP cells and add 15 mL of prewarmed (37 °C) RPMI 1640 medium with 10% fetal bovine serum (FBS) in a T75 culture flask. Keep the cells growing in a temperature-controlled cell culture incubator at 37 °C with 5% CO₂. Replace the complete medium at least 2x a week.

NOTE: Do not disturb the cell growth and keep checking the cell growing conditions daily. The cells need to be subcultured when they reach 85%–90% confluency to maintain the proliferation phase.

1.2. One week before the cell implantation step, remove the puromycin from the cell culture flask by first removing all the medium in the culture flask, then rinsing 2x with 10 mL of 1x phosphate buffered saline (PBS), and finally replacing the medium with complete medium without the puromycin. During the medium-adding and rinsing steps, do not disturb the cells. Remember not to use the complete medium with the selection antibiotics from now on for all medium replenishment steps.

1.3. On the day of preparing the cells for implantation, remove all complete medium before trypsinization to avoid deactivating the trypsin. Add 5 mL of trypsin to the flask to trypsinize the cells. Monitor the cells and check that they detach from the culture flask.

1.4. Once the majority of the cells detach, add 10 mL of complete medium to neutralize the trypsin activity. Next, transfer the cell suspension to a 50 mL centrifuge tube and centrifuge at $\sim 150 \times g$ to pellet the cells. Remove the supernatant after the centrifugation and then add 10 mL of 1x PBS to resuspend the cells and prepare for cell counting.

1.5. Count the cells with a cell counter and adjust the cell concentration to 7.5×10^6 cells/mL in cold 1x PBS containing 10% basement membrane matrix. Prepare 7.5×10^5 cells in 0.1 mL 1x PBS with 10% basement membrane matrix for injection into the fourth mammary fat pad of each mouse. Bring extra needles and syringes for the cell implantation and keep the cell-basement-membrane-matrix mix on ice prior to implantation.

NOTE: There is dead space in the syringe and needle. Depending on the choice of needle and syringe length, type, and size, a tuberculin syringe with a 0.5 in 26 G needle can have up to 70 µL dead space¹⁰. Prepare 40%–50% more cell implantation mix to compensate for the dead space and any other accidental loss.

2. Orthotopic breast cancer model and tumor size measurement

2.1. Allow 6-week-old female athymic nude mice to acclimate to the housing facility for at least 1 week before the cell implantation.

NOTE: Using same age mice will reduce data variation.

2.2. For each round, anesthetize five mice with isoflurane at 4% with filtered (0.2 µm) air at a flow rate of 1 L/min for 3–4 min. Pay attention to the mouse respiratory rate and pattern change, and use a toe pinch to ensure that the mice are under proper anesthesia. Once they are no longer moving, remove one mouse and place a nose cone over its nose and mouth with the same anesthesia.

2.3. Swab the left 4th mammary gland with alcohol. Using fine rat tooth forceps, lift the 4th mammary gland slightly to insert the 25 G needle. Make sure the needle is bevel up and then slightly pull the plunger to make sure the needle does not hit any blood vessels. If no blood enters the syringe, continue to slowly inject 100 µL of the cell-basement-membrane-matrix mix into the mammary fat pad.

NOTE: A round, raised area will appear underneath the skin.

2.4. Wait 10–15 s for the basement membrane matrix to harden, then remove the needle. Repeat the process with the remaining mice in the induction chamber. Place all used needles and syringes in a sharp box.

2.5. Use the same mammary gland injection site for all mice. Keep a close eye on the injection site and note any cell implantation mix leaking out from the injection site.

NOTE: Within a few minutes, the mouse will start to regain consciousness.

2.6. Allow the xenograft to grow freely without any interruption for 7–10 days prior to any tumor size measurement.

2.7. Examine all mice for the xenograft size. Measure the tumor size with a caliper. Determine the tumor volume (mm³) with the following equation:

$$\frac{L \times W \times W}{2} = Tumor\ Volume$$

where L is the longest dimension and W is the shortest dimension perpendicular to L.

2.8. Identify and remove outliers exceeding one standard deviation of the mean. Only use mice with comparable tumor sizes for experiments. Randomly divide the mice into different treatment groups and begin treatments.

2.9. Measure the tumor size by caliper 2x a week. Keep note of all the physical changes of the xenografts (i.e., necrosis, laceration).

3. In vivo bioluminescence and ex vivo fluorescence imaging

NOTE: In this study, both two-dimensional bioluminescence and fluorescence imaging are conducted at the endpoint of the experiment. The bioluminescence imaging (BLI) was performed using a commercial preclinical optical scanner equipped with a 16-bit cooled CCD camera and heated imaging stage.

3.1. Before imaging, anesthetize up to five tumor-bearing mice in the induction chamber by setting isoflurane at 3% with filtered (0.2 μ m) air at a flow rate of 1 L/min for 3–4 min. Determine anesthesia by a toe pinch. Ensure that the induction chamber is kept inside a vented hood to minimize staff exposure to isoflurane.

3.2. Administer D-luciferin (150 mg/kg) to the anesthetized mice by an intraperitoneal route using a 27 G needle, and transfer an anesthetized mouse to the imaging chamber. At the scanner imaging chamber, maintain the isoflurane at 2%–2.5% with O₂ as a carrier with a flow rate of 1 L/min.

NOTE: Maintain the body temperature of the mouse at ~37 °C during the procedure by keeping a heated pad under the anesthesia induction chamber, imaging table (if the stage is not heated), and postprocedure recovery cage.

3.3. Before imaging the study mice, obtain luciferin kinetics by imaging three extra tumor bearing mice (animals not assigned to any study groups) at 2 min intervals for a total of 40 min using the following parameters: excitation filter-blocked, emission filter-open, f/stop 1, FOV-D, medium binning (8 x 8), and auto exposure. Use the peak bioluminescence signal measured to define the optimal image acquisition time window for all subsequent time points.

3.4. While performing metastasis imaging, shield the high BLI signal from the primary tumor by covering it with a sleeve cut out from a black glove. Acquire the image using the same parameters described in step 3.3 with the ventral side of the mouse facing the camera for lung metastasis imaging and the dorsal side of the mouse facing the camera for the brain metastasis imaging.

NOTE: It is essential to test a few different brands of black gloves to pick the one with minimal auto luminescence.

3.5. Using a scanner and data analysis software, draw a standard shape region of interest (ROI) over the thoracic cavity or the brain ensuring that the entire organ of interest is covered to evaluate the metastatic burden. Quantify the bioluminescence (BL) output as total flux (photons/second).

3.6. Immediately after BLI, euthanize the mouse via CO₂ asphyxiation (as per ACUC guidelines and institution-approved animal protocols) and extract the lung and the brain with dissecting scissors and forceps for ex vivo imaging.

NOTE: The lung extracted for ex vivo imaging and for lung metastasis nodule counting cannot be performed on the same mouse due to incompatible procedures.

3.7. Quickly rinse all organs with 1x PBS to remove any superficial bloodstains and place organs on a low-autofluorescence, black plastic plate. Transport organs to a multispectral fluorescence scanner equipped with spectral unmixing capability (solid-state liquid crystal wavelength tuning) with a 12-bit CCD camera for GFP detection.

3.8. Acquire multispectral GFP images (excitation filter = 457 ± 23 nm; emission filter = 490 nm long pass) of the extracted organs and non-tumor bearing control mice by scanning through 500–720 nm at a step size of 10 nm. Use excised organs from non-tumor bearing control mice to correct for autofluorescence.

3.9. After multispectral GFP imaging, determine the optimal imaging settings. Perform image acquisition of all target organs and conduct image analysis (i.e., generate a spectral library for autofluorescence and GFP for spectral unmixing procedure) according to the manufacturer's protocol.

4. Molecular detection of metastatic breast cancer cells

4.1. After the ex vivo imaging, snap freeze the whole brain in liquid nitrogen and store at -80 °C in a freezer until ready for the DNA extraction.

4.2. For DNA extraction, put the whole brain in a 5 mL homogenizing tube with 2 mL of DNA lysis buffer. Use a homogenizer with the power setting at 50 to homogenize the snap-frozen whole brain tissue. Once the brain tissue is totally homogenized, transfer the 1 mL suspension (lysate) to a DNase-free and RNase-free 2 mL microcentrifuge tube and continue to isolate the DNA according to the manufacturer's protocol.

NOTE: To minimize carryover DNA contamination, thoroughly clean the homogenizer after each sample by first rinsing it with 75% ethanol in DNase-free and RNase-free water, then rinsing with 1 M NaOH solution, followed by a rinse with 75% ethanol in DNase-free and RNase-free water to effectively reduce and destroy any DNA residue.

4.3. Add 0.5 mL of 100% ethanol of DNA lysis buffer to the lysate. Mix sample by inversion and store at room temperature for 3 min.

NOTE: Do not invert too many times or too vigorously. The DNA will be visible as a wool-like precipitate.

4.4. Use a pipette tip to transfer the DNA to a fresh DNase-free and RNase-free 2 mL microcentrifuge tube. Let the sample air dry for 1 min. Add 1 mL 75% ethanol and invert the microcentrifuge tube 3–6x to wash the DNA sample. Discard the ethanol after each wash by pipetting. Repeat the wash step 2x.

4.5. Air dry the DNA sample for 10 s. Then add 52 µL of 8 mM NaOH to dissolve the DNA sample. Pipet 2 µL of the DNA sample for DNA quantitation, and use the rest 50 µL for a real-time PCR assay after concentration adjustment.

NOTE: NaOH helps to fully solubilize the DNA sample.

4.6. Quantitate 2 µL of each DNA sample with a spectrophotometer and use an absorbance ratio between A₂₆₀/A₂₈₀ as a quality check reference. Calculate the DNA concentration with this formula:

$$\text{dsDNA concentration} = 50 \mu\text{g/mL} \times \text{OD}_{260} \times \text{dilution factor}$$

4.7. Adjust the DNA concentration to 50 ng/µL. For each DNA sample, use 50 ng of DNA as the starting template for a real-time PCR assay. Use 8 mM NaOH solution or DNase-free and RNase-free water to dilute the DNA sample.

4.8. Design the primer pair specific to the exogenous green fluorescence protein (GFP) sequence in-house using an open source primer design web portal for real-time PCR detection of the GFP tag in the metastatic cells that invaded and colonized distal sites.

NOTE: This study used F: 5'-AGAACGGCATCAAGGTGAAC-3', R: 5'-TGCTCAGGTAGTGGTTGTCG-3'.

4.9. Use a fast real-time PCR reagent and a real-time PCR machine that supports a fast real-time PCR protocol. In addition to the regular 30 cycle amplification steps, add a dissociation curve step to the end of the run for the detection of any nonspecific amplification.

NOTE: The following conditions were used for molecular detection: 95 °C 2 min hot start, 40 cycles of 95 °C 5 s, 60 °C 15 s, and lastly a melt curve analysis. The GFP amplicon is 135 bp in size.

4.10. Use a naive mouse brain DNA (not a MDA-MB-231 cell implant) as a negative control. Use DNA extracted from the MDA-MB-231-GFP/Luc cells as a positive control. Add all the PCR reagents without any DNA template as a no template control (NTC).

NOTE: A PCR control is needed for each PCR assay.

5. Metastatic breast cancer cell detection in lung

5.1. For the mice subgroup chosen for the metastatic lung nodule counting, anesthetize mice with isoflurane (as in step 2.2) immediately after the ex vivo imaging, perform a cardiac puncture for blood collection, and then euthanize by cervical dislocation.

5.2. Open the chest cavity with dissecting scissors and cut past the heart and thymus to expose the trachea.

5.3. Insert a 10 mL syringe with a 22 G needle containing Bouin's solution into the trachea. Push the syringe plunger until the collapsed lungs are swollen with ~2 mL of the Bouin's solution. Remove the syringe and needle once the lungs have been inflated.

5.4. Place the whole lung into a 15 mL tube containing Bouin's solution, gently invert the tube a few times, and allow to soak for 24 h at room temperature.

5.5. After 24 h, remove the Bouin's solution from the tube, rinse the lung with water, and then place it back in the tube with 70% ethanol. Count metastasis (white patches or nodules) on the surfaces of the lungs using a dissecting microscope.

6. Data collection and analysis

6.1. Record tumor volume data, as well as in vivo and ex vivo imaging data, on an electronic spreadsheet for easy data entry, collection, and management.

6.2. At the end of the experiment, transfer all data to the electronic spreadsheet and statistical software for data plotting and statistical analyses.

REPRESENTATIVE RESULTS:

Tumor volume measurement by caliper is a well-established method to assess treatment efficacy (**Figure 1**). The number of cells implanted, use of basement membrane matrix, microbiome, facility cleanliness, and injection site are the key factors impacting the tumor growth rate.

Unlike the GFP imaging, BLI required the administration of luciferase substrate at least 15–20 min prior to BLI imaging. Furthermore, the mouse strain, cell line, treatments, and luciferase reporter all affect the bioluminescence signal levels. Thus, to obtain comparable signals between the study groups, a pre-imaging BLI kinetic study must be conducted to determine the best imaging time frame (**Figure 2**).

Due to the superior signal-to-background ratio^{27,28}, the whole body in vivo bioluminescence imaging was quite sensitive in detecting low-level metastasis signal compared to the GFP approach (**Figure 3**). Furthermore, the bioluminescence signal provided deeper penetration than

GFP by a few millimeters. However, bioluminescence signal production requires ATP, which is a limiting factor in evaluating ex vivo tissue samples. If the animals are processed quickly, then BLI could be a viable approach to obtain quantitative results on metastasis. One way to achieve this is by processing one animal at a time. However, this approach was not feasible for this study because a large cohort of mice was used. BLI signal was not detected when the organs were imaged around 45 min post luciferin injection. The use of a dual reporter cell line is useful in this situation. Due to the stable nature of the GFP molecule, researchers would have sufficient time to process the carcass prior to capturing the GFP signals from target organs (**Figure 4**).

Figure 5 provides a real-life example of how caliper tumor size measurements could distort the data interpretation, because the xenograft lost most of the viable tumor cell content but still maintained its large mass and shape. Histopathological examination of those xenografts indicated necrosis inside the mass (**Figure 5B**).

For researchers who challenge the imaging results regarding the brain metastasis in the orthotopic breast cancer model, molecular detection by real-time PCR can provide convincing evidence (**Figure 6**). In this case, the exogenous GFP DNA sequence was the best way to address this problem, because the transfected GFP DNA sequence does not naturally exist in humans or rodents.

FIGURE LEGENDS:

Figure 1: Tumor volume measurement. Tumor volume/loading measurement with a caliper started on day 10 after xenograft implantation and then was measured 2x a week until the end of the experiment. Error bars are calculated by SEM value.

Figure 2: Determination of optimal image acquisition window. Left: One mouse with a large xenograft and one mouse with a small xenograft were selected for the optimal luciferin kinetic range determination. Right: Luciferin kinetic curve obtained by acquiring the images every 2 min for 40 min. A plateau was observed between 15–22 min, which was used as an optimal image acquisition time for all subsequent imaging.

Figure 3: Whole body BLI imaging. L: Whole body BLI imaging. M: Ventral view with the lower body covered with a sleeve of a black glove. R: Dorsal view with the lower body covered with a sleeve of a black glove. An axillary lymph node metastasis is detected in the ventral view by BLI imaging.

Figure 4: Ex vivo BLI/GFP signal detection. GFP signals were detected in the brain and lung from the same mouse 20 min after the mouse was sacrificed. BLI signal was not detected 45 min post luciferin injection. No GFP signal was detected in naive mouse brain and lung.

Figure 5: Advantages of optical imaging techniques over caliper measurements. (A) Representative image showing in vivo GFP signal detection in a primary tumor. Only a minor portion of the xenograft showed GFP signal, suggesting that a significant portion of the mass was stroma. This cannot be determined by traditional caliper measurements and can lead to an

inaccurate conclusion. This example highlights the importance of optical imaging for the animal model study. **(B)** Histopathology section of the same mouse showing that the necrotic region (i.e., inner region) also contributed to the tumor size calculation.

Figure 6: Melt curve analysis. The melt curve plot showing the specificity of GFP amplicons. DNA from the brain obtained from the MDA-MB-231-Luc/GFP-implanted mice and the DNA isolated from the MDA-MB-231-Luc/GFP cells grown in culture (positive control) were assayed. The real-time PCR assay was performed to assess the GFP content in the brain tissue. **(A,B)** The melting curves of the positive control and the DNA extracted from mouse brain, respectively. **(C)** The overlapped curves of panels A and B, indicating the peak signals from the mouse brain DNAs are specific for the exogenous GFP sequence.

DISCUSSION:

For the study of TNBC in animals, two murine models have been developed: the MDA-MB-231 human breast adenocarcinoma cells in immune-compromised mice (i.e. athymic nude mice, NSG mice), and the 4T1 in immune-competent BALB/c mice. Both models have their advantages. The choice of the animal model for a study depends on the research goals. For example, the MDA-MB-231 model is a human TNBC cell line grown in immunocompromised mice that mimics immunosuppressed human breast cancer patients. On the other hand, the invasive phenotype of orthotopic 4T1 triple-negative murine breast cancer cells in BALB/c mice closely mimics the metastatic process as it occurs in stage IV human breast cancer patients. Unlike the intravenous cell injection approach, human MDA-MB-231 breast cancer cells were similarly injected into the mammary fat pad^{11,12} in the orthotopic breast cancer model^{11,13}. The longer tumor growth and the acquired metastatic ability is more physiologically relevant, thus it is not an artificial metastatic cancer model^{4,14}. Such a spontaneous metastasis model closely mimics human breast cancer development except for the initiation stage. This is a crucial model for in vivo drug screening and therapeutic efficacy assessment in metastatic breast cancer.

The tumor implantation site in the mouse plays a crucial role in providing a microenvironment that sustains tumor growth and the selection of metastatic phenotype similar to that which occurs in humans. The proximal lymph node and the presence of adipose tissue are the key factors affecting the disease progression of breast cancer^{15,16}. In a human patient, the lymph node and adipose tissue are both key interacting factors affecting the malignancy and incidence of breast cancer¹⁷⁻¹⁹. Thus, the selection of the correct anatomical location for the injection site can highly impact the relevancy of the tumor model compared to the human disease. This study used the fourth mammary gland as the implantation site mainly due to the aforementioned requirements and that it is anatomically more accessible and easier to manipulate.

Different tumor volume calculation methods are available, and a researcher can choose any they see fit. The algorithm selected for this study is based on the findings by Faustino-Rocha et al., who compared different tumor volume calculation formulas and concluded that the formula below is the most accurate²⁰.

$$\frac{L \times W \times W}{2} = Tumor Volume$$

Basement membrane matrix is an important extracellular matrix used in various in vitro²¹ and in vivo^{22,23} assays. There are contradicting reports^{22,24,25} regarding the influence of the basement membrane matrix on xenograft malignancy. It seems to only affect the initial establishment of the xenograft and have no further effect on xenograft growth²⁵. For the xenograft implantation described, the basement membrane matrix was mixed with the cancer cells to increase the cell/gel mix solution viscosity prior to implantation. The presence of the basement membrane matrix reduces the loss of mix solution from the injection site and keeps the mix solution at the implantation site, thus increasing the uniformity of the implanted xenograft volume.

The MDA-MB-231 cell line is a malignant immortalized human breast adenocarcinoma cell line and is a popular tool in breast cancer research because of its triple-negative status. The use of dual reporters (luciferase and GFP) cell line allows more flexibility in handling the in vivo and ex vivo imaging. It is well established that the bioluminescence signal possesses greater sensitivity, depth detectability, and superior contrast (signal-to-noise ratio) than GFP signals. Because of this, it is a widely used imaging modality for whole body imaging. Unfortunately, bioluminescence detection is limited by a narrow time window (~15–20 mins post luciferin injection) during which the signal detection is linear. BLI signal diminishes rapidly when the animals are euthanized. This becomes an experimental design issue if many mice need to be euthanized and harvesting multiple tissues or organs is required. In these studies, blood was harvested by direct heart puncture, the brain, primary tumor, lung, and affected lymph node were examined in 40 mice. By the time the organs were harvested and ready for ex vivo imaging, the bioluminescence signal was undetectable. Therefore, GFP detection is more suitable in these situations. The emission of the GFP signal is in the visible range, and at these wavelengths, signal absorption due to blood (i.e., hemoglobin) is significantly higher. Also, autofluorescence in the visible range due to NADH, lipo-pigments, and flavins results in a significant background that makes it difficult to distinguish between a low-level GFP signal and autofluorescence background. Employing a multispectral fluorescence imaging approach instead of traditional filter-pair imaging and using spectral unmixing algorithms helps identify true GFP signal in the organ of interest. Hence, by combining the strengths of bioluminescence imaging in whole body in vivo detection and multispectral GFP imaging in the ex vivo organ/tissue evaluations, quantifiable data can be maximized in a large cohort of mice.

No matter which approach is selected for an animal study, extracting all blood prior to organ/tissue retrieval is highly recommended, especially for studies targeting the metastatic burden. This protocol detects GFP signals from the whole blood samples obtained from the mice

(data not shown) in the orthotopic breast cancer model by real-time PCR assays. Minimizing the blood volume in organs/tissues will reduce the false positive signal in the target organs.

In conclusion, the orthotopic breast cancer model using the MDA-MB-231-Luc/GFP cells is a highly relevant animal model that closely mimics the human TNBC patient condition. This model is essential for studying, monitoring, and assessing therapeutic efficacy in a tumor microenvironment similar to human beings. The use of dual reporter cell lines further enhances the practicality of this orthotopic breast cancer model.

ACKNOWLEDGMENTS:

The authors would like to acknowledge support by the Intramural Research Program of the National Institutes of Health, National Cancer Institute, Bethesda MD, Cancer and Inflammation Program, and the Frederick National Laboratory - Small Animal Imaging Program, Leidos Biomedical Research, Inc, Frederick Maryland, USA.

DISCLOSURES:

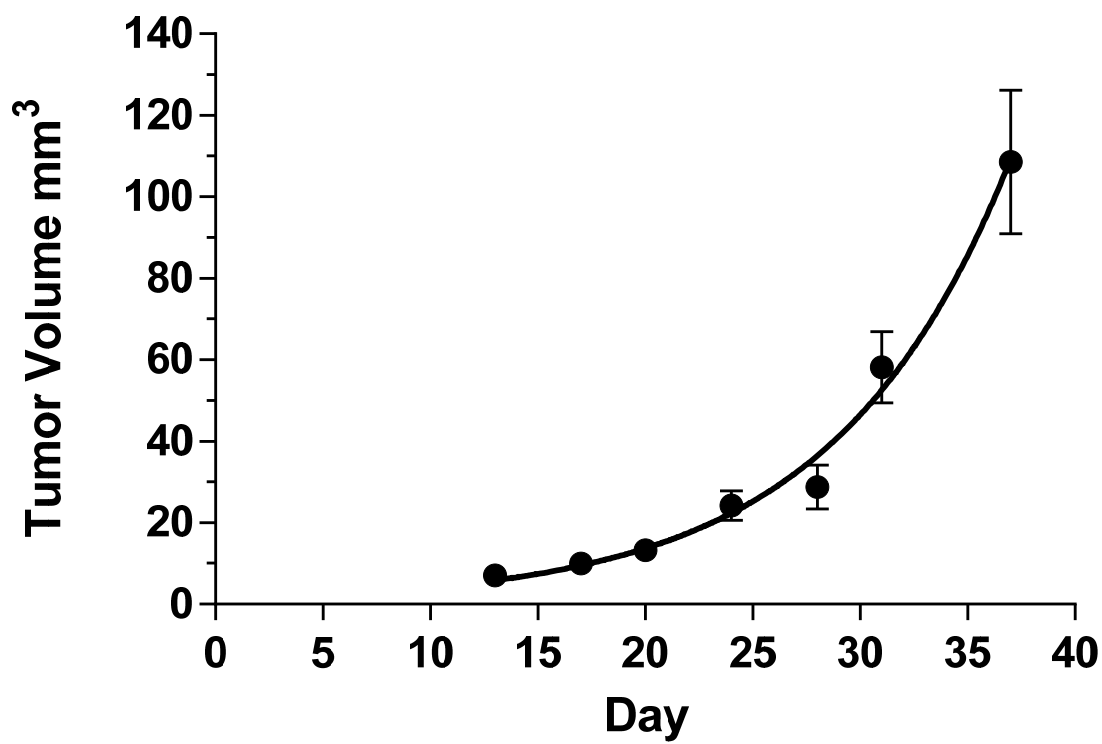
The authors have nothing to disclose.

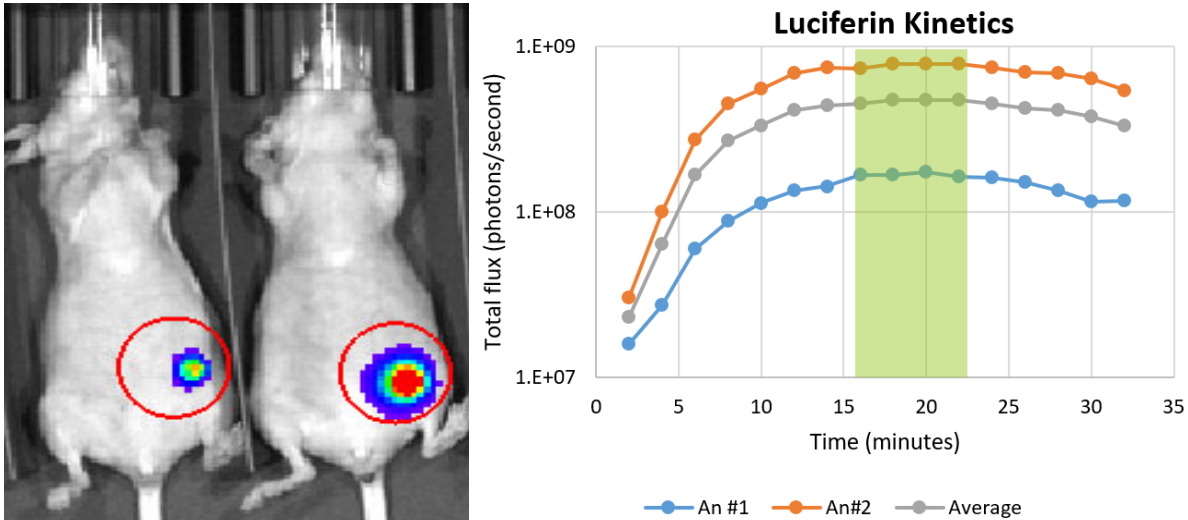
REFERENCES:

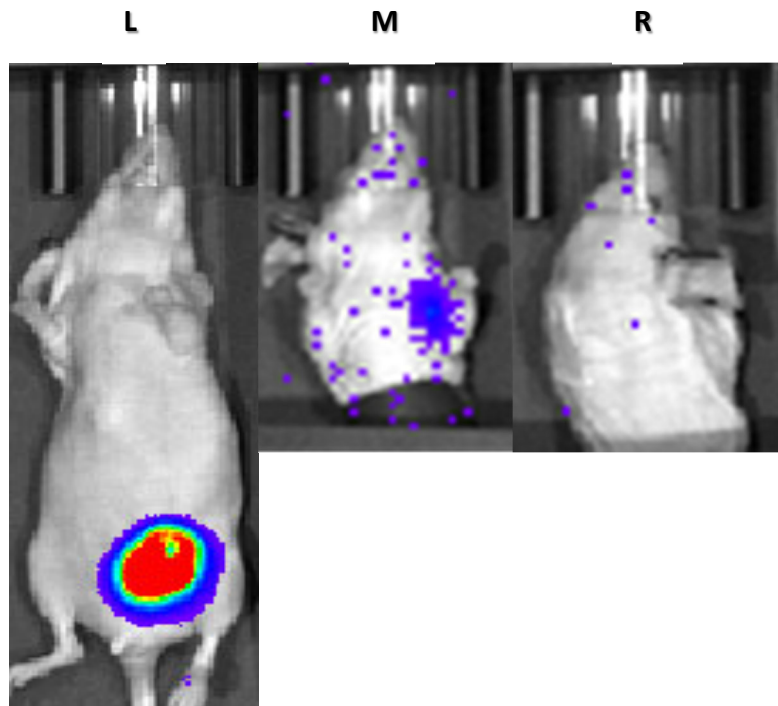
1. Abramson V. G., Lehmann B. D., Ballinger T. J., Pietersen J. A. Subtyping of triple-negative breast cancer: implications for therapy. *Cancer*. **121**, 8–16 (2015).
2. Zhuang X., Zhang H., Hu G. Cancer and Microenvironment Plasticity: Double-Edged Swords in Metastasis. *Trends in Pharmacological Sciences*. **40** (6), 419–429 (2019).
3. Campbell J. P., Merkel A. R., Masood-Campbell S. K., Eleftheriou F., Sterling J. A. Models of bone metastasis. *Journal of Visualized Experiment*. (67), e4260 (2012).
4. Saha D., et al. In vivo bioluminescence imaging of tumor hypoxia dynamics of breast cancer brain metastasis in a mouse model. *Journal of Visualized Experiment*. (56), e3175 (2011).
5. Goddard E. T., Fischer J., Schedin P. A Portal Vein Injection Model to Study Liver Metastasis of Breast Cancer. *Journal of Visualized Experiment*. (118), e54903 (2016).
6. Lim E. et al. Monitoring tumor metastases and osteolytic lesions with bioluminescence and micro CT imaging. *Journal of Visualized Experiment*. (50), e2775 (2011).
7. Bauerle T., Komljenovic D., Berger M. R., Semmler W. Multi-modal imaging of angiogenesis in a nude rat model of breast cancer bone metastasis using magnetic resonance imaging, volumetric computed tomography and ultrasound. *Journal of Visualized Experiment*. (66), e4178 (2012).
8. Katsuta E., Oshi M., Rashid O. M., Takabe K. Generating a Murine Orthotopic Metastatic Breast Cancer Model and Performing Murine Radical Mastectomy. *Journal of Visualized Experiment*. (141), e57849 (2018).
9. Rashid O. M. et al. Is tail vein injection a relevant breast cancer lung metastasis model? *Journal of Thoracic Disease*. **5**, 385–392 (2013).
10. Bhambhani V., Beri R.S., Puliyl J.M. Inadvertent overdosing of neonates as a result of the dead space of the syringe hub and needle. *Archives of Disease in Childhood: Fetal and Neonatal Edition*. **90**, F444–445 (2005).
11. Zhang G. L., Zhang Y., Cao K. X., Wang X. M. Orthotopic Injection of Breast Cancer Cells into the Mice Mammary Fat Pad. *Journal of Visualized Experiment*. (143), e58604 (2019).
12. Tavera-Mendoza L. E., Brown M. A less invasive method for orthotopic injection of breast cancer cells into the mouse mammary gland. *Laboratory Animals*. **51**, 85–88 (2017).

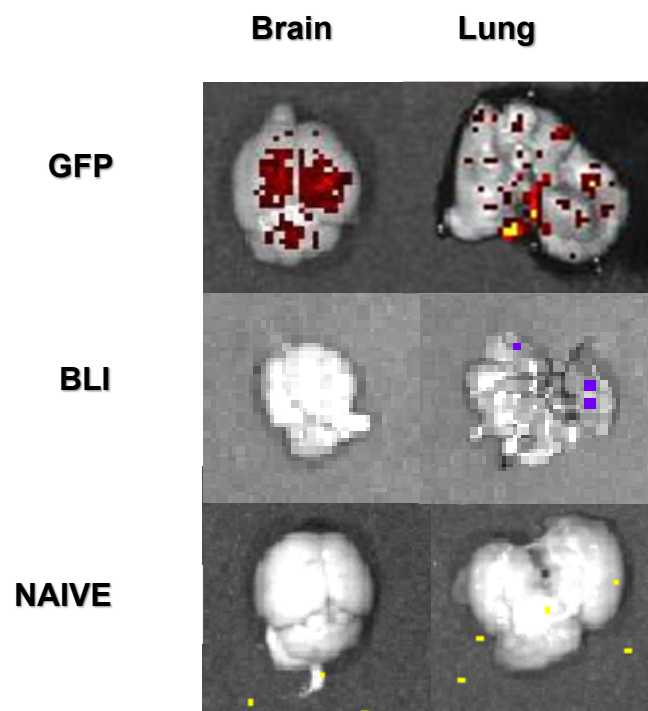
13. Paschall A. V., Liu K. An Orthotopic Mouse Model of Spontaneous Breast Cancer Metastasis. *Journal of Visualized Experiment*. (114), e54040 (2016).
14. Kocaturk B., Versteeg H. H. Orthotopic injection of breast cancer cells into the mammary fat pad of mice to study tumor growth. *Journal of Visualized Experiment*. (96), e51967 (2015).
15. Fletcher S. J., et al. Human breast adipose tissue: characterization of factors that change during tumor progression in human breast cancer. *Journal of Experimental and Clinical Cancer Research*. **36**, 26 (2017).
16. Giuliano A. E., et al. Axillary dissection vs no axillary dissection in women with invasive breast cancer and sentinel node metastasis: a randomized clinical trial. *Journal of the American Medical Association*. **305**, 569–575 (2011).
17. Rummel S., Hueman M. T., Costantino N., Shriver C. D., Ellsworth R. E. Tumour location within the breast: Does tumour site have prognostic ability? *Ecancermedicalscience*. **9**, 552 (2015).
18. Kroman N., Wohlfahrt J., Mouridsen H. T., Melbye M. Influence of tumor location on breast cancer prognosis. *International Journal of Cancer*. **105**, 542–545 (2003).
19. Bao J., Yu K. D., Jiang Y. Z., Shao Z. M., Di G. H. The effect of laterality and primary tumor site on cancer-specific mortality in breast cancer: a SEER population-based study. *PLoS One*. **9**, e94815 (2014).
20. Faustino-Rocha A. et al. Estimation of rat mammary tumor volume using caliper and ultrasonography measurements. *Lab Animal*. **42**, 217–224 (2013).
21. Mullen P. The use of Matrigel to facilitate the establishment of human cancer cell lines as xenografts. *Methods in Molecular Medicine*. **88**, 287–292 (2004).
22. Jensen R. L., Leppla D., Rokosz N., Wurster R. D. Matrigel augments xenograft transplantation of meningioma cells into athymic mice. *Neurosurgery*. **42**, 130–135; discussion 135–136 (1998).
23. Mullen P., Langdon S. P. The use of matrigel in the establishment of ovarian carcinoma cell lines as xenografts. *Methods in Molecular Medicine*. **39**, 199–203 (2001).
24. Fliedner F. P., Hansen A. E., Jorgensen J. T., Kjaer A. The use of matrigel has no influence on tumor development or PET imaging in FaDu human head and neck cancer xenografts. *BMC Medical Imaging*. **16**, 5 (2016).
25. Mullen P., Ritchie A., Langdon S. P., Miller W. R. Effect of Matrigel on the tumorigenicity of human breast and ovarian carcinoma cell lines. *International Journal of Cancer*. **67**, 816–820 (1996).

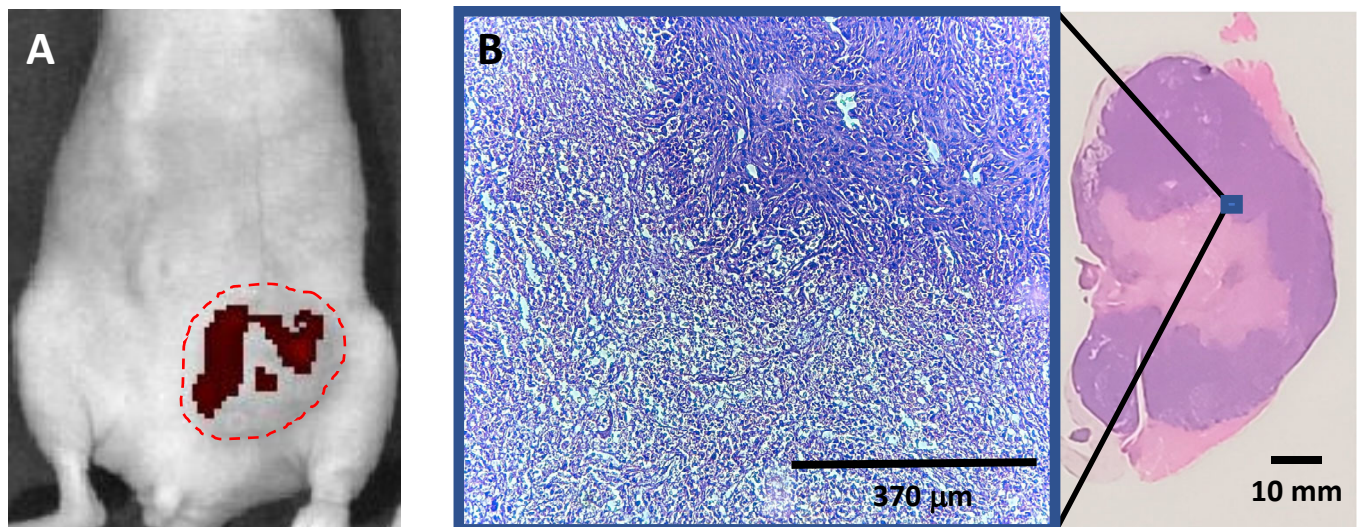
MDA-MB-231 Tumor Growth

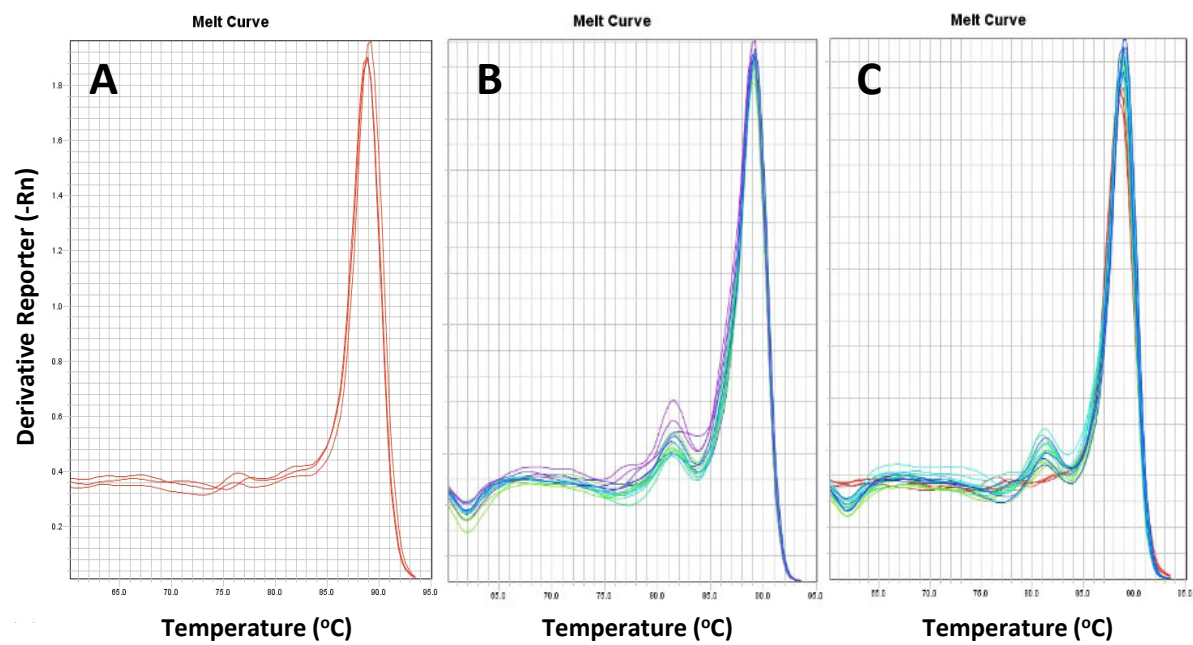












Name of Material/ Equipment	Company	Catalog Number	Comments/Description
Bouins Solution	Sigma	HT10132-1L	Lung metastatic nodule staining
D-Luciferin, Potassium Salt	GoldBio	LUCK-1G	Luciferase substrate
DNAzol	ThermoFisher	10503027	DNA extraction Kit
Excel	Microsoft		Spreadsheet software
homogenizer	Virtis	Cyclone Virtishear	For tissue homogenization
IVIS SPECTRUM scanner	Perkin Elmer		fluorescence and BLI imaging system
Maestro GNIR- FLEX fluorescence	Perkin Elmer		fluorescence imaging system
MatriGel Matrix	Corning	356234	Store at -20C and keep old (4 C) when in use.
MDA-MB-231 / Luciferase-2A-GFP	GenTarget	SC044	Dual Reporter human breast cancer cell line
Microscope	ThermoFisher	EVOS	histology image capture
Phosphate-Buffered	ThermoFisher	10010049	rinse buffer
Primer3	MIT		Primer Design
Prism	GraphPad		Statistical Analysis Software
Puromycin	ThermoFisher	A1113803	Antibiotics
RPMI 1640 media	ThermoFisher	61870127	Culture media
SeniFAST SYBR Lo- ROX kit	Bioline	BIO-94020	Fast Real-Time PCR Reagent
StepOne Plus Real- Time PCR system	ThermoFisher		Real-Time PCR machine

ARTICLE AND VIDEO LICENSE AGREEMENT

Title of Article:	A Practical Guide to Study Triple Negative Breast Cancer Using Orthotopic Breast Cancer Model
Author(s):	Cheng, RYS; Patel, N; Back, T; Basudhar, D; Somasundaram, V; Kalen, J; Wink, DA; Ridnour, LA

Item 1: The Author elects to have the Materials be made available (as described at <http://www.jove.com/publish>) via:

☐

Standard Access

☒

Open Access

Item 2: Please select one of the following items:

☐

The Author is **NOT** a United States government employee.

☒

The Author is a United States government employee and the Materials were prepared in the course of his or her duties as a United States government employee.

☐

The Author is a United States government employee but the Materials were NOT prepared in the course of his or her duties as a United States government employee.

ARTICLE AND VIDEO LICENSE AGREEMENT

1. **Defined Terms.** As used in this Article and Video License Agreement, the following terms shall have the following meanings: “**Agreement**” means this Article and Video License Agreement; “**Article**” means the article specified on the last page of this Agreement, including any associated materials such as texts, figures, tables, artwork, abstracts, or summaries contained therein; “**Author**” means the author who is a signatory to this Agreement; “**Collective Work**” means a work, such as a periodical issue, anthology or encyclopedia, in which the Materials in their entirety in unmodified form, along with a number of other contributions, constituting separate and independent works in themselves, are assembled into a collective whole; “**CRC License**” means the Creative Commons Attribution-Non Commercial-No Derivs 3.0 Unported Agreement, the terms and conditions of which can be found at: <http://creativecommons.org/licenses/by-nc-nd/3.0/legalcode>; “**Derivative Work**” means a work based upon the Materials or upon the Materials and other pre-existing works, such as a translation, musical arrangement, dramatization, fictionalization, motion picture version, sound recording, art reproduction, abridgment, condensation, or any other form in which the Materials may be recast, transformed, or adapted; “**Institution**” means the institution, listed on the last page of this Agreement, by which the Author was employed at the time of the creation of the Materials; “**JOVE**” means MyJove Corporation, a Massachusetts corporation and the publisher of The Journal of Visualized Experiments; “**Materials**” means the Article and / or the Video; “**Parties**” means the Author and JOVE; “**Video**” means any video(s) made by the Author, alone or in conjunction with any other parties, or by JOVE or its affiliates or agents, individually or in collaboration with the Author or any other parties, incorporating all or any portion

of the Article, and in which the Author may or may not appear.

2. **Background.** The Author, who is the author of the Article, in order to ensure the dissemination and protection of the Article, desires to have the JOVE publish the Article and create and transmit videos based on the Article. In furtherance of such goals, the Parties desire to memorialize in this Agreement the respective rights of each Party in and to the Article and the Video.

3. **Grant of Rights in Article.** In consideration of JOVE agreeing to publish the Article, the Author hereby grants to JOVE, subject to **Sections 4** and **7** below, the exclusive, royalty-free, perpetual (for the full term of copyright in the Article, including any extensions thereto) license (a) to publish, reproduce, distribute, display and store the Article in all forms, formats and media whether now known or hereafter developed (including without limitation in print, digital and electronic form) throughout the world, (b) to translate the Article into other languages, create adaptations, summaries or extracts of the Article or other Derivative Works (including, without limitation, the Video) or Collective Works based on all or any portion of the Article and exercise all of the rights set forth in (a) above in such translations, adaptations, summaries, extracts, Derivative Works or Collective Works and (c) to license others to do any or all of the above. The foregoing rights may be exercised in all media and formats, whether now known or hereafter devised, and include the right to make such modifications as are technically necessary to exercise the rights in other media and formats. If the “Open Access” box has been checked in **Item 1** above, JOVE and the Author hereby grant to the public all such rights in the Article as provided in, but subject to all limitations and requirements set forth in, the CRC License.

ARTICLE AND VIDEO LICENSE AGREEMENT

4. **Retention of Rights in Article.** Notwithstanding the exclusive license granted to JoVE in **Section 3** above, the Author shall, with respect to the Article, retain the non-exclusive right to use all or part of the Article for the non-commercial purpose of giving lectures, presentations or teaching classes, and to post a copy of the Article on the Institution's website or the Author's personal website, in each case provided that a link to the Article on the JoVE website is provided and notice of JoVE's copyright in the Article is included. All non-copyright intellectual property rights in and to the Article, such as patent rights, shall remain with the Author.

5. **Grant of Rights in Video – Standard Access.** This **Section 5** applies if the "Standard Access" box has been checked in **Item 1** above or if no box has been checked in **Item 1** above. In consideration of JoVE agreeing to produce, display or otherwise assist with the Video, the Author hereby acknowledges and agrees that, Subject to **Section 7** below, JoVE is and shall be the sole and exclusive owner of all rights of any nature, including, without limitation, all copyrights, in and to the Video. To the extent that, by law, the Author is deemed, now or at any time in the future, to have any rights of any nature in or to the Video, the Author hereby disclaims all such rights and transfers all such rights to JoVE.

6. **Grant of Rights in Video – Open Access.** This **Section 6** applies only if the "Open Access" box has been checked in **Item 1** above. In consideration of JoVE agreeing to produce, display or otherwise assist with the Video, the Author hereby grants to JoVE, subject to **Section 7** below, the exclusive, royalty-free, perpetual (for the full term of copyright in the Article, including any extensions thereto) license (a) to publish, reproduce, distribute, display and store the Video in all forms, formats and media whether now known or hereafter developed (including without limitation in print, digital and electronic form) throughout the world, (b) to translate the Video into other languages, create adaptations, summaries or extracts of the Video or other Derivative Works or Collective Works based on all or any portion of the Video and exercise all of the rights set forth in (a) above in such translations, adaptations, summaries, extracts, Derivative Works or Collective Works and (c) to license others to do any or all of the above. The foregoing rights may be exercised in all media and formats, whether now known or hereafter devised, and include the right to make such modifications as are technically necessary to exercise the rights in other media and formats. For any Video to which this **Section 6** is applicable, JoVE and the Author hereby grant to the public all such rights in the Video as provided in, but subject to all limitations and requirements set forth in, the CRC License.

7. **Government Employees.** If the Author is a United States government employee and the Article was prepared in the course of his or her duties as a United States government employee, as indicated in **Item 2** above, and any of the licenses or grants granted by the Author hereunder exceed the scope of the 17 U.S.C. 403, then the rights granted hereunder shall be limited to the maximum

rights permitted under such statute. In such case, all provisions contained herein that are not in conflict with such statute shall remain in full force and effect, and all provisions contained herein that do so conflict shall be deemed to be amended so as to provide to JoVE the maximum rights permissible within such statute.

8. **Protection of the Work.** The Author(s) authorize JoVE to take steps in the Author(s) name and on their behalf if JoVE believes some third party could be infringing or might infringe the copyright of either the Author's Article and/or Video.

9. **Likeness, Privacy, Personality.** The Author hereby grants JoVE the right to use the Author's name, voice, likeness, picture, photograph, image, biography and performance in any way, commercial or otherwise, in connection with the Materials and the sale, promotion and distribution thereof. The Author hereby waives any and all rights he or she may have, relating to his or her appearance in the Video or otherwise relating to the Materials, under all applicable privacy, likeness, personality or similar laws.

10. **Author Warranties.** The Author represents and warrants that the Article is original, that it has not been published, that the copyright interest is owned by the Author (or, if more than one author is listed at the beginning of this Agreement, by such authors collectively) and has not been assigned, licensed, or otherwise transferred to any other party. The Author represents and warrants that the author(s) listed at the top of this Agreement are the only authors of the Materials. If more than one author is listed at the top of this Agreement and if any such author has not entered into a separate Article and Video License Agreement with JoVE relating to the Materials, the Author represents and warrants that the Author has been authorized by each of the other such authors to execute this Agreement on his or her behalf and to bind him or her with respect to the terms of this Agreement as if each of them had been a party hereto as an Author. The Author warrants that the use, reproduction, distribution, public or private performance or display, and/or modification of all or any portion of the Materials does not and will not violate, infringe and/or misappropriate the patent, trademark, intellectual property or other rights of any third party. The Author represents and warrants that it has and will continue to comply with all government, institutional and other regulations, including, without limitation all institutional, laboratory, hospital, ethical, human and animal treatment, privacy, and all other rules, regulations, laws, procedures or guidelines, applicable to the Materials, and that all research involving human and animal subjects has been approved by the Author's relevant institutional review board.

11. **JoVE Discretion.** If the Author requests the assistance of JoVE in producing the Video in the Author's facility, the Author shall ensure that the presence of JoVE employees, agents or independent contractors is in accordance with the relevant regulations of the Author's institution. If more than one author is listed at the beginning of this Agreement, JoVE may, in its sole

ARTICLE AND VIDEO LICENSE AGREEMENT

discretion, elect not take any action with respect to the Article until such time as it has received complete, executed Article and Video License Agreements from each such author. JoVE reserves the right, in its absolute and sole discretion and without giving any reason therefore, to accept or decline any work submitted to JoVE. JoVE and its employees, agents and independent contractors shall have full, unfettered access to the facilities of the Author or of the Author's institution as necessary to make the Video, whether actually published or not. JoVE has sole discretion as to the method of making and publishing the Materials, including, without limitation, to all decisions regarding editing, lighting, filming, timing of publication, if any, length, quality, content and the like.

12. **Indemnification.** The Author agrees to indemnify JoVE and/or its successors and assigns from and against any and all claims, costs, and expenses, including attorney's fees, arising out of any breach of any warranty or other representations contained herein. The Author further agrees to indemnify and hold harmless JoVE from and against any and all claims, costs, and expenses, including attorney's fees, resulting from the breach by the Author of any representation or warranty contained herein or from allegations or instances of violation of intellectual property rights, damage to the Author's or the Author's institution's facilities, fraud, libel, defamation, research, equipment, experiments, property damage, personal injury, violations of institutional, laboratory, hospital, ethical, human and animal treatment, privacy or other rules, regulations, laws, procedures or guidelines, liabilities and other losses or damages related in any way to the submission of work to JoVE, making of videos by JoVE, or publication in JoVE or elsewhere by JoVE. The Author shall be responsible for, and shall hold JoVE harmless from, damages caused by lack of sterilization, lack of cleanliness or by contamination due to

the making of a video by JoVE its employees, agents or independent contractors. All sterilization, cleanliness or decontamination procedures shall be solely the responsibility of the Author and shall be undertaken at the Author's expense. All indemnifications provided herein shall include JoVE's attorney's fees and costs related to said losses or damages. Such indemnification and holding harmless shall include such losses or damages incurred by, or in connection with, acts or omissions of JoVE, its employees, agents or independent contractors.

13. **Fees.** To cover the cost incurred for publication, JoVE must receive payment before production and publication the Materials. Payment is due in 21 days of invoice. Should the Materials not be published due to an editorial or production decision, these funds will be returned to the Author. Withdrawal by the Author of any submitted Materials after final peer review approval will result in a US\$1,200 fee to cover pre-production expenses incurred by JoVE. If payment is not received by the completion of filming, production and publication of the Materials will be suspended until payment is received.

14. **Transfer, Governing Law.** This Agreement may be assigned by JoVE and shall inure to the benefits of any of JoVE's successors and assignees. This Agreement shall be governed and construed by the internal laws of the Commonwealth of Massachusetts without giving effect to any conflict of law provision thereunder. This Agreement may be executed in counterparts, each of which shall be deemed an original, but all of which together shall be deemed to be one and the same agreement. A signed copy of this Agreement delivered by facsimile, e-mail or other means of electronic transmission shall be deemed to have the same legal effect as delivery of an original signed copy of this Agreement.

A signed copy of this document must be sent with all new submissions. Only one Agreement is required per submission.

CORRESPONDING AUTHOR

Name:	Lisa A. Ridnour
Department:	Cancer and Inflammation Program
Institution:	National Cancer Institute at Frederick
Title:	Dr.
Signature:	<div>Ridnour, Lisa (NIH/NCI) [E]</div> <div>Digitally signed by Ridnour, Lisa (NIH/NCI) [E] Date: 2019.05.24 11:36:37 -04'00'</div>

Please submit a **signed** and **dated** copy of this license by one of the following three methods:

1. Upload an electronic version on the JoVE submission site
2. Fax the document to +1.866.381.2236
3. Mail the document to JoVE / Attn: JoVE Editorial / 1 Alewife Center #200 / Cambridge, MA 02140

First, we would like to thank you for the reviewer's comments and questions. By incorporating the suggestions and comments from the reviewers, it really strengthened our manuscript. Below are our responses to the reviewer's comments and questions.

Editorial comments:

1. Please take this opportunity to thoroughly proofread the manuscript to ensure that there are no spelling or grammar issues. The JoVE editor will not copy-edit your manuscript and any errors in the submitted revision may be present in the published version.

Response: We have proofread the manuscript.

2. Authors and affiliations: Please provide an email address for each author.

Response: Email address added for each author.

3. Please add a Summary section before the Abstract section to clearly describe the protocol and its applications in complete sentences between 10–50 words: "Here, we present a protocol to ..."

Response: Summary section added.

4. JoVE cannot publish manuscripts containing commercial language. This includes trademark symbols (™), registered symbols (®), and company names before an instrument or reagent. Please remove all commercial language from your manuscript and use generic terms instead. All commercial products should be sufficiently referenced in the Table of Materials. You may use the generic term followed by "(Table of Materials)" to draw the readers' attention to specific commercial names. Examples of commercial sounding language in your manuscript are: PerkinElmer Inc., IVIS SPECTRUM, Living Image, Maestro software, etc.

Response: Brand names are replaced with generic names.

5. Please adjust the numbering of the Protocol to follow the JoVE Instructions for Authors. Step 1 followed by 1.1, followed by 1.1.1, etc. Each step should include 1–2 actions and contain 2–3 sentences. Use subheadings and substeps for clarity if there are discrete stages in the protocol. Please refrain from using bullets, dashes, or indentations.

Response: Manuscript updated to JoVE format.

6. Please revise the Protocol to contain only action items that direct the reader to do something (e.g., "Do this," "Ensure that," etc.). The actions should be described in the imperative tense in complete sentences wherever possible. Avoid usage of phrases such as "could be," "should be," and "would be" throughout the Protocol. Any text that cannot be written in the imperative tense may be added as a "NOTE." Please include all safety procedures and use of hoods, etc. However, notes should be used sparingly and actions should be described in the imperative tense wherever possible. Please move the discussion about the protocol to the Discussion.

Response: Imperative tense is adopted in the revised manuscript.

7. Please add more details to your protocol steps. There should be enough detail in each step to supplement the actions seen in the video so that viewers can easily replicate the protocol. Please ensure you answer the “how” question, i.e., how is the step performed? Alternatively, add references to published material specifying how to perform the protocol action. See examples below.

Response: Detail steps were added.

8. Lines 89-91: Please describe how the cells are transfected.

Response: Cells were a commercial product, we did not transfect those cells. We noted in the protocol that those cells are purchased from a vendor.

9. Lines 92-93: At what conditions are the cells grown? What container is used?

Response: Growing conditions and container information are added.

10. Line 94: How to remove puromycin from the medium?

Response: Puromycin rinsing steps are added.

11. Line 96: Please describe how to trypsinize cells.

Response: Detail trypsinization steps are added.

12. Line 98: What volume of PBS is used to rinse?

Response: 10 ml 1X PBS information is added.

13. Lines 109-110: Please mention how animals are anesthetized and how proper anesthetization is confirmed.

Response: Detailed steps on anesthetizing the mice and testing the depth of anesthesia are added.

14. Please ensure that the manuscript is formatted according to JoVE guidelines—letter (8.5” x 11”) page size, 1-inch margins, 12 pt Calibri font throughout, all text aligned to the left margin, single spacing within paragraphs, and single-line spaces between all paragraphs and protocol steps/substeps. Do not underline any text in the protocol.

Response: Page margins are formatted according to JoVE’s guideline.

15. Please combine some of the shorter Protocol steps so that individual steps contain 2-3 actions and maximum of 4 sentences per step.

Response: Shorter steps are combined.

16. After you have made all the recommended changes to your protocol section (listed above), please highlight in yellow up to 2.75 pages (no less than 1 page) of protocol text (including

headers and spacing) to be featured in the video. Bear in mind the goal of the protocol and highlight the critical steps to be filmed. Our scriptwriters will derive the video script directly from the highlighted text.

Response: Text highlighted.

17. Please highlight complete sentences (not parts of sentences). Please ensure that the highlighted steps form a cohesive narrative with a logical flow from one highlighted step to the next. The highlighted text must include at least one action that is written in the imperative voice per step. Notes cannot usually be filmed and should be excluded from the highlighting.

Response: Sentence highlighted.

18. Please include all relevant details that are required to perform the step in the highlighting. For example: If step 2.5 is highlighted for filming and the details of how to perform the step are given in steps 2.5.1 and 2.5.2, then the sub-steps where the details are provided must be highlighted.

Response: Relevant detail steps are highlighted.

19. Please do not highlight any steps describing anesthetization and euthanasia.

Response: None of the anesthetization and euthanasia steps are highlighted.

20. Please upload each Figure individually to your Editorial Manager account as a .png, .tiff, .pdf, .svg, .eps, .psd, or .ai file.

Response: Figures are saved in PDF format individually.

21. Please remove the titles and figure legends from the uploaded figures. Please include all the figure Legends together at the end of the Representative Results in the manuscript text.

Response: Titles and figure legends are moved after the Representative Results section.

22. Please use superscript arabic numerals to cite references in text. The superscript number is inserted immediately next to the word/group of words it applies to but before any punctuation.

Response: Reference fonts and format updated as suggested

23. References: Please do not abbreviate journal titles; use full journal name.

Response: Reference journal names are expanded to full names.

Reviewers' comments:

Reviewer #1:

Manuscript Summary:

The manuscript accurately describes the assay and discusses the strengths and weaknesses within the assay. The authors also discuss the advantages of using IVIS and fluorescence based methods to detect tumor and metastases both in vivo and ex vivo. Lastly, the authors discuss how this assay could be applied to better the field.

Response: Thank you for the comments.

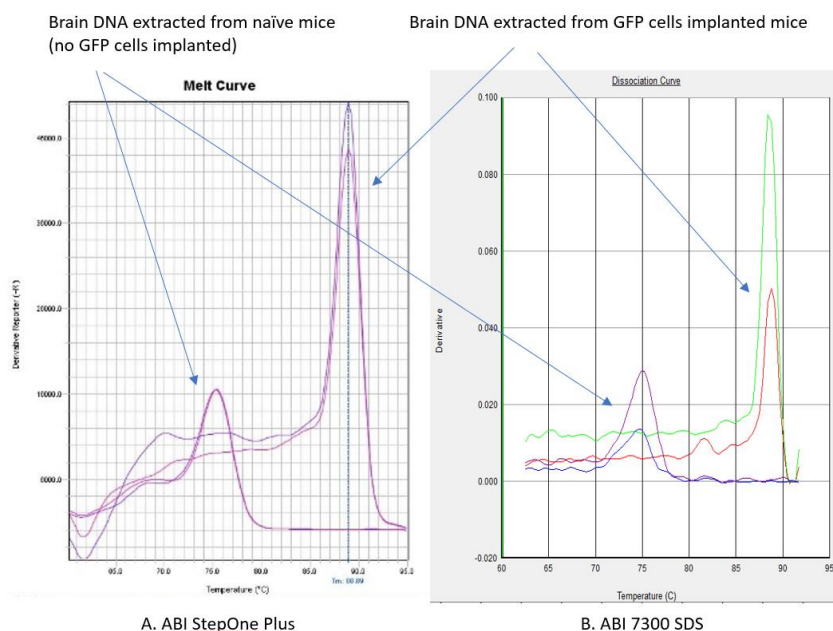
Major Concerns:

No major concerns.

Minor Concerns:

It would be helpful to reader to address a couple of minor concerns. Figure 6 does not show the most accurate data for what they are trying to show, although it is fully believable that this method would work. While they show the melt curve for cells grown in culture and cells isolated from mice, they are lacking the amplification curves and a negative control (ex. brain tissue from a mouse that did not have cancer cells implanted).

Response:



Thank you for the comments. The above melt curves are coming from two different real-time PCR machines and reagents (A & B) shows the same GFP peaks location (close to 90C). The minor peaks close to 75C are the non-specific amplification from the naive mice brain tissue (no GFP cells implanted).

The amplification plot is designed to provide an amplicon's abundance information and the result is easily affected by non-specific amplification or the presence of contaminants. In this case, our GFP primer pair does induce a minor non-specific amplification and that's why we do not consider the amplification plot is that useful. And that's why we omit it from this protocol and use the melt curve instead because of its high specificity. Also, the melt curve can provide a reference peak (close to 90C) for any researcher which is willing to use our GFP primer pair. In our hand, the GFP peak locations remain at a constant coordination in different PCR settings and studies.

It would also help the readers to better show the specificity of the primers (and publish the primer sequences) by showing non-GFP samples (i.e. negative control) are not amplified with the GFP primers.

Response: The GFP primer pair sequence is included in the protocol.

In figure 5 they show only part of the tumor has GFP cells by IVIS and say the rest of the mass was stroma (figure legend) or necrosis (representative results section) and this makes perfect sense, however it would be helpful to show the histopathological sections they referred to in the text so the readers can see the stroma or necrosis.

Response: Thank you for the comment and suggestion. A histopathological figure is added to demonstrate the area without fluorescent signals in the xenograft.

Figure 4 addresses the time constraints of bioluminescence signal ex vivo and shows GFP is much more stable than bioluminescence, which is true. However, it is unclear if the brain and lungs used in these figures are the same. If not, it would be better to show the GFP and bioluminescence in the same brain and same lung.

Response: Thank you for the comment. We didn't make it clear in the original manuscript. The brain and lung images are coming from the same mice in each group. We have added the mice's information in the context.

Reviewer #2:

Manuscript Summary:

Agree with the rationale for orthotopic implantation metastatic process as opposed to injection

To have a protocol for accurately evaluating the metastatic patterns for TNBC is necessary in investigating growth and metastatic inhibitory therapy. This is a positive impact.

The use of scanning for lung and brain metastasis before sacrificing the animal will decrease the number of animal necessary to assess the metastatic process compared to euthanizing. DNA analysis of the brain to assess TNBC metastasis as opposed to scanning for visual identification may prove quite a unique method of assessment since visualization to count brain metastasis would prove difficult

Response: Thank you for the comments.

May add significantly to the armamentarium of the researcher studying TNBC

Major Concerns:

The researchers never explained why they use the 4th mammary fat pad.

Response: Physio-anatomical location and physical accessibility are the two main reasons supporting the decision to use that site. Implanting the xenograft on the left or right side does not matter, as long as all animals involved using the same side. This explanation is added to the context.

Page 6, line 105 seem like a lot of extra volume of 40-50% to compensate for dead space in the needle and syringe. The author should explain the actual volume numerically as opposed to percent

Response: The exact dead space volume information was added to the protocol. The reason for using the percentage is because not everyone using the same brand/size/length of syringe and needle.

Explain the tumor volume calculation and why the division by 2 since the usual calculation is $L \times W \times H$ or $L \times 2W$ to get volume in mm^3 .

Response: We adopted this formula from the Faustino-Rocha A et al publication. They compared different tumor size calculation and determined this is the most accurate formula.

Discuss the consideration of the effect of injecting matrigel into the body of the mice and potential limitation to in vivo growth of the tumor

Response: The discussion of the effects and limitations of matrigel were added to the discussion.

Minor Concerns:

Typographical errors:

Response: All typo errors are corrected.

Abstract

Line 36... delete the duplicate "are"

Introduction

Page 3, line 57... "within" one word.

Page 3, line 59... word is "common" not "commonly"

Page 4, line 76... breast cancer "(MDA-MB-231)" corrected

Page 7, line 134...delete "with"

Page 8, line 153... abbreviation "BL" should be written out somewhere prior to its first use

Page 10, line 186... abbreviation "GFP" should be written out somewhere prior to its first use

Page 14, line 250...injected "into" the mammary fat